

Extreme trans-Neptunian objects and the Kozai mechanism: signaling the presence of trans-Plutonian planets?

C. de la Fuente Marcos* and R. de la Fuente Marcos

Universidad Complutense de Madrid, Ciudad Universitaria, E-28040 Madrid, Spain

Accepted 2014 June 3. Received 2014 June 3; in original form 2014 April 23

ABSTRACT

The existence of an outer planet beyond Pluto has been a matter of debate for decades and the recent discovery of 2012 VP₁₁₃ has just revived the interest for this controversial topic. This Sedna-like object has the most distant perihelion of any known minor planet and the value of its argument of perihelion is close to 0°. This property appears to be shared by almost all known asteroids with semimajor axis greater than 150 au and perihelion greater than 30 au (the extreme trans-Neptunian objects or ETNOs), and this fact has been interpreted as evidence for the existence of a super-Earth at 250 au. In this scenario, a population of stable asteroids may be shepherded by a distant, undiscovered planet larger than the Earth that keeps the value of their argument of perihelion librating around 0° as a result of the Kozai mechanism. Here, we study the visibility of these ETNOs and confirm that the observed excess of objects reaching perihelion near the ascending node cannot be explained in terms of any observational biases. This excess must be a true feature of this population and its possible origin is explored in the framework of the Kozai effect. The analysis of several possible scenarios strongly suggest that at least two trans-Plutonian planets must exist.

Key words: celestial mechanics – minor planets, asteroids: general – minor planets, asteroids: individual: 2012 VP₁₁₃ – planets and satellites: individual: Neptune.

1 INTRODUCTION

Are there any undiscovered planets left in the Solar system? The answer to this question is no and perhaps yes! If we are talking about planets as large as Jupiter or Saturn moving in nearly circular orbits with semimajor axes smaller than a few dozen thousand astronomical units, the answer is almost certainly negative (Luhman 2014). However, smaller planets orbiting the Sun well beyond Neptune may exist and still avoid detection by current all-sky surveys (see e.g. Sheppard et al. 2011). Nevertheless, the answer to the question is far from settled and the existence of an outer planet located beyond Pluto has received renewed attention in recent years (see e.g. Gomes, Matese & Lissauer 2006; Lykawka & Mukai 2008; Fernández 2011; Iorio 2011, 2012; Matese & Whitmire 2011). So far, the hunt for a massive trans-Plutonian planet has been fruitless.

The recent discovery of 2012 VP₁₁₃ (Sheppard & Trujillo 2014), a probable dwarf planet that orbits the Sun far beyond Pluto, has further revived the interest in this controversial subject. Trujillo & Sheppard (2014) have suggested that nearly 250 au from the Sun lies an undiscovered massive body, probably a super-Earth with up to ten times the mass of our planet. This claim is based on circumstantial evidence linked to the discovery of 2012 VP₁₁₃ that has the most distant perihelion of any known object. The value of the argument of perihelion of this Sedna-like object is close to

0°. This property appears to be shared by almost all known asteroids with semimajor axis greater than 150 au and perihelion greater than 30 au (the extreme trans-Neptunian objects or ETNOs), and this has been interpreted as evidence for the existence of a hidden massive perturber. In this scenario, a population of asteroids could be shepherded by a distant, undiscovered planet larger than the Earth that keeps the value of their argument of perihelion librating around 0° as a result of the Kozai mechanism. The Kozai mechanism (Kozai 1962) protects the orbits of high inclination asteroids from close encounters with Jupiter but it also plays a role on the dynamics of near-Earth asteroids (Michel & Thomas 1996).

Trujillo & Sheppard (2014) claim that the observed excess of objects reaching perihelion near the ascending node cannot be the result of observational bias. In this Letter, we study the visibility of extreme trans-Neptunian objects and the details of possible observational biases. Our analysis confirms the interpretation presented in Trujillo & Sheppard (2014) and uncovers a range of additional unexpected patterns in the distribution of the orbital parameters of the ETNOs. The overall visibility is studied in Section 2 using Monte Carlo techniques and an obvious intrinsic bias in declination is identified. The impact of the bias in declination is analyzed in Section 3. The distribution in orbital parameter space of real objects is shown in Section 4. In Section 5, our findings are analyzed within the context of the Kozai resonance. Results are discussed in Section 6 and conclusions are summarized in Section 7.

* E-mail: nbplanet@fis.ucm.es

2 VISIBILITY OF TRANS-NEPTUNIAN OBJECTS: A MONTE CARLO APPROACH

Trujillo & Sheppard (2014) focused their discussion on asteroids with perihelion greater than 30 au and semimajor axis in the range 150–600 au. Here, we study the visibility of these ETNOs as seen from our planet. The actual distribution of the orbital elements of objects in this population is unknown. In the following, we will assume that the orbits of these objects are uniformly distributed in orbital parameter space. This is the most simple choice and, by comparing with real data, it allows the identification of observational biases and actual trends easily. Using a Monte Carlo approach, we create a synthetic population of ETNOs with semimajor axis, $a \in (150, 600)$ au, eccentricity, $e \in (0, 0.99)$, inclination, $i \in (0, 90)^\circ$, longitude of the ascending node, $\Omega \in (0, 360)^\circ$, and argument of perihelion, $\omega \in (0, 360)^\circ$. We restrict the analysis to objects with perigee < 90 au. Out of this synthetic population we single out those objects with perihelion, $q = a(1 - e) > 30$ au, nearly 20 per cent of the sample. Both, the test and Earth’s orbit are sampled in phase space until the minimal distance or perigee is found (that is sometimes but not always near perihelion due to the relative geometry of the orbits). Twenty million test orbits were studied. We do not assume any specific size (absolute magnitude) distribution because its nature is also unknown and we are not interested in evaluating any detection efficiency. In principle, our results are valid for both large primordial objects and those (likely smaller) from collisional origin. Further details of our technique can be found in de la Fuente Marcos & de la Fuente Marcos (2014a, b).

Fig. 1 shows the distribution in equatorial coordinates of the studied test orbits at perigee. In this figure, the value of the parameter in the appropriate units is colour coded following the scale printed on the associated colour box. Both perigees (panel A) and semimajor axes (panel B) are uniformly distributed. The eccentricity (panel C) is always in the range 0.4–0.95. Inclination (panel D), longitude of the ascending node (panel E) and argument of perihelion (panel F) exhibit regular patterns. The frequency distribution in equatorial coordinates (see Fig. 2) shows a rather uniform behaviour in right ascension, α ; in contrast, most of the objects reach perigee at declination, δ , in the range -24° to 24° . Therefore, and assuming a uniform distribution for the orbital parameters of objects in this population, there is an intrinsic bias in declination induced by our observing point on Earth. Under the assumptions made here, this intrinsic bias and any secondary biases induced by it are independent on how far from the ecliptic the observations are made. In other words, if the objects do exist and their orbits are uniformly distributed in orbital parameter space, most objects will be discovered at $|\delta| < 24^\circ$ no matter how complete and extensive the surveys are. But, what is the expected impact of this intrinsic bias on the observed orbital elements?

3 THE IMPACT OF THE DECLINATION BIAS

So far, all known trans-Neptunian objects with $q > 30$ au had $|\delta| < 24^\circ$ at discovery which supports our previous result (see Table 1 and Fig. 2). But this intrinsic bias may induce secondary biases on the observed orbital elements. If we represent the frequency distribution in right ascension and the orbital parameters a , e , i , Ω and ω for test orbits with $|\delta| < 24^\circ$, we get Fig. 3. Out of an initially almost uniform distribution in α , i , Ω and ω (see Figs 2 and A1), we obtain biased distributions in all these four parameters. In contrast, the distributions in a and e are rather unaffected (other than

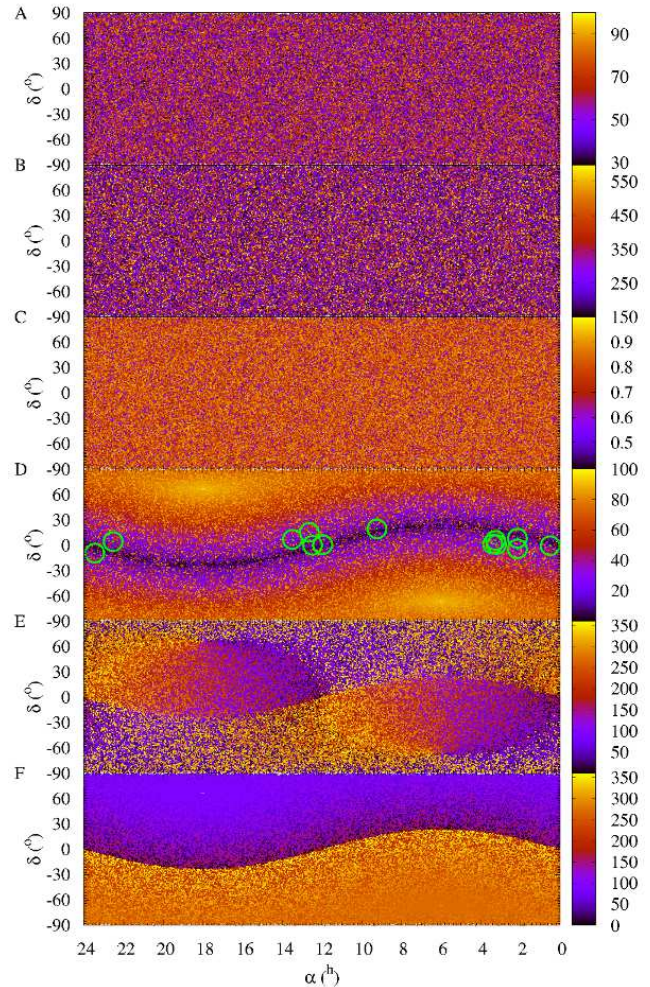


Figure 1. Distribution in equatorial coordinates of the studied test orbits at perigee as a function of various orbital elements and parameters. As a function of the perigee of the candidate (panel A); as a function of a (panel B); as a function of e (panel C); as a function of i (panel D); as a function of Ω (panel E); as a function of ω (panel F). The associated frequency distributions are plotted in Fig. A1. The green circles in panel D give the location at discovery of all the known objects (see Table 1).

scale factors) by the intrinsic bias in δ . Therefore, most objects in this population should be discovered with semimajor axes near the low end of the distribution, eccentricities in the range 0.8–0.9, inclinations under 40° , longitude of the ascending node near 180° , and argument of perihelion preferentially near 0° and 180° . Any deviation from these expected secondary biases induced by the intrinsic bias in declination will signal true characteristic features of this population. Therefore, we further confirm that the clustering in ω pointed out by Trujillo & Sheppard (2014) is real, not the result of observational bias. Unfortunately, the number of known objects is small (13), see Table 1, and any conclusions obtained from them will be statistically fragile.

4 DISTRIBUTION IN ORBITAL PARAMETER SPACE OF REAL OBJECTS

The distribution in orbital parameter space of the objects in Table 1 shows a number of puzzling features (see Fig. 3). In addi-

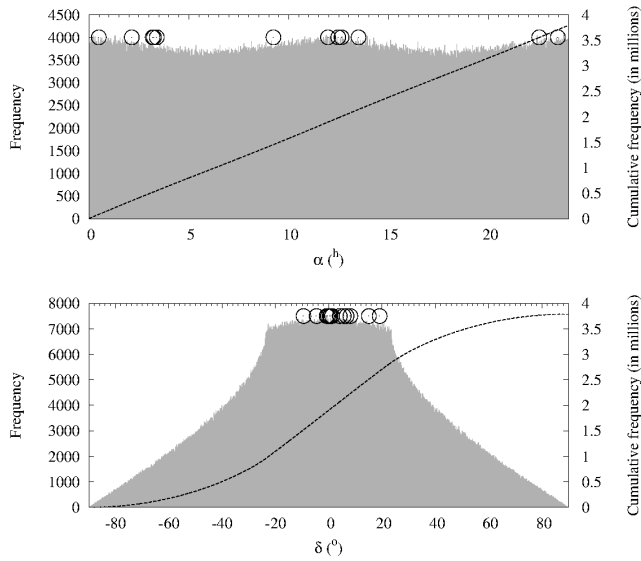


Figure 2. Frequency distribution in equatorial coordinates (right ascension, top panel, and declination, bottom panel) of the studied test orbits at perigee. The distribution is rather uniform in right ascension and shows a maximum for declinations in the range -24° to 24° . The bin sizes are 0.024 hours in right ascension and $0^\circ.18$ in declination, error bars are too small to be seen. The black circles correspond to objects in Table 1.

tion to the clustering of ω values around 0° (but not 180°) already documented by Trujillo & Sheppard (2014), we observe clustering around 20° in inclination and, perhaps, around 120° in longitude of the ascending node. The distributions in right ascension, semimajor axis and eccentricity of known objects appear to be compatible with the expectations. However, (90377) Sedna and 2007 TG₄₂₂ are very clear outliers in semimajor axis. Their presence may signal the existence of a very large population of similar objects, the inner Oort cloud (Brown, Trujillo & Rabinowitz 2004). The distribution in inclination is also particularly revealing. Such a clustering in inclination closely resembles the one observed in the inner edge of the main asteroid belt for the Hungaria family (see e.g. Milani et al. 2010). Consistently, some of these objects could be submitted to an approximate mean motion resonance with an unseen planet. In particular, the orbital elements of 82158 and 2002 GB₃₂ are very similar. On the other hand, asteroids 2003 HB₅₇, 2005 RH₅₂ and 2010 VZ₉₈ all have similar a , e and i , and their mean longitudes, λ , differ by almost 120° (see Table A1). This feature reminds us of the Hildas, a dynamical family of asteroids trapped in a 3:2 mean motion resonance with Jupiter (see e.g. Brož & Vokrouhlický 2008). If the three objects are indeed trapped in a 3:2 resonance with an unseen perturber, it must be moving in an orbit with semimajor axis in the range 195–215 au. This automatically puts the other two objects, with semimajor axis close to 200 au, near the 1:1 resonance with the hypothetical planet. Their difference in λ is also small (see Table A1), typical of Trojans or quasi-satellites. Almost the same can be said about 2003 SS₄₂₂ and 2007 VJ₃₀₅. The difference in λ between these two pairs is nearly 180° . On the other hand, the clustering of ω values around 0° could be the result of a Kozai resonance (Kozai 1962). An argument of perihelion librating around 0° means that these objects reach perihelion at approximately the same time they cross the ecliptic from South to North (librating around 180° implies that the perihelion is close to the descending node). When the Kozai resonance occurs at low inclinations, the argument of perihelion librates around 0° or 180° (see e.g. Milani et

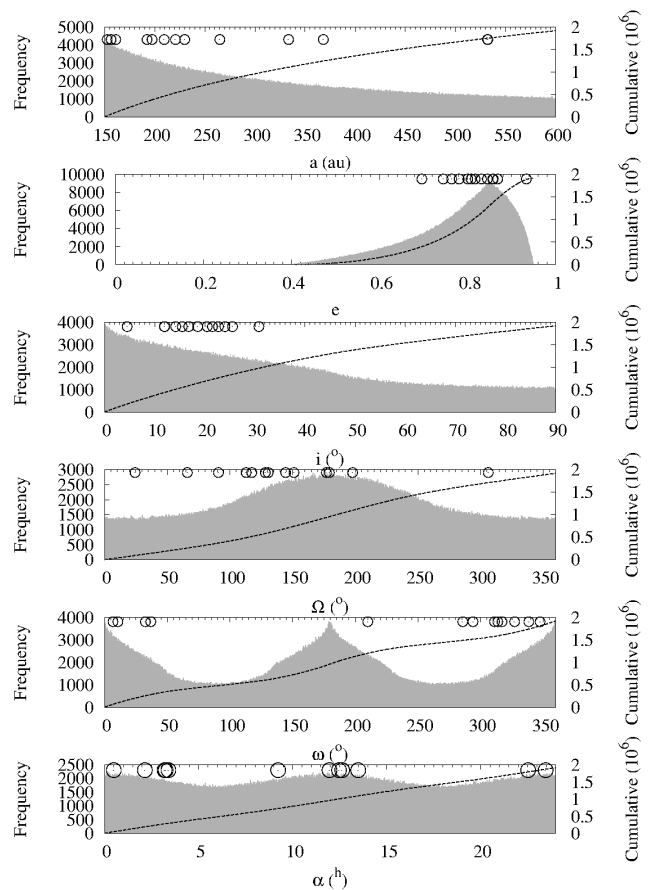


Figure 3. Frequency distribution in right ascension (bottom panel) and the orbital elements of test orbits with $|\delta| < 24^\circ$. The bin sizes are 0.45 au in semimajor axis, 0.001 in eccentricity, $0^\circ.09$ in inclination, $0^\circ.36$ in longitude of the node, $0^\circ.36$ in argument of perihelion and 0.024 hours in right ascension, error bars are too small to be seen. The black circles correspond to objects in Table 1. Data from Table A1 have been used.

al. 1989). At the Kozai resonance, the precession rate of its argument of perihelion is nearly zero. This resonance provides a temporary protection mechanism against close encounters with planets. An object locked in a Kozai resonance is in a metastable state, where it can remain for a relatively long amount of time before a close encounter with a planet drastically changes its orbit.

5 DIFFERENT KOZAI SCENARIOS

The most typical Kozai scenario is characterized by the presence of a primary (the Sun in our case), the perturbed body (a massless test particle, an asteroid) and a massive outer or inner perturber such as the ratio of semimajor axes (perturbed vs. perturber) tends to zero (for an outer perturber) or infinity (for an inner perturber). In the case of an outer perturber, the critical inclination angle separating the circulation and libration regimes is $\sim 39^\circ$; for an inner perturber it is $\sim 63^\circ$ (see e.g. Gallardo, Hugo & Pais 2012). Here, the libration occurs at $\omega = 90^\circ$ and 270° . Under these circumstances, aphelion (for the outer perturber) or perihelion (for the inner perturber) always occur away from the orbital plane of the perturber. This lack of encounters greatly reduces or completely halts any diffusion in semimajor axis. A classical example of an object submitted to the Kozai effect induced by an outer perturber is the asteroid

Table 1. Equatorial coordinates, apparent magnitudes (with filter if known) at discovery time, absolute magnitude, and ω for the 13 objects discussed in this paper. (J2000.0 ecliptic and equinox. Source: MPC Database.)

Object	α (h:m:s)	δ (°:′:″)	m (mag)	H (mag)	ω (°)
(82158) 2001 FP ₁₈₅	11:57:50.69	+00:21:42.7	22.2 (R)	6.0	6.77
(90377) Sedna	03:15:10.09	+05:38:16.5	20.8 (R)	1.5	311.19
(148209) 2000 CR ₁₀₅	09:14:02.39	+19:05:58.7	22.5 (R)	6.3	317.09
2002 GB ₃₂	12:28:25.94	-00:17:28.4	21.9 (R)	7.7	36.89
2003 HB ₅₇	13:00:30.58	-06:43:05.4	23.1 (R)	7.4	10.64
2003 SS ₄₂₂	23:27:48.15	-09:28:43.4	22.9 (R)	7.1	209.98
2004 VN ₁₁₂	02:08:41.12	-04:33:02.1	22.7 (R)	6.4	327.23
2005 RH ₅₂	22:31:51.90	+04:08:06.1	23.8 (g)	7.8	32.59
2007 TG ₄₂₂	03:11:29.90	-00:40:26.9	22.2	6.2	285.84
2007 VJ ₃₀₅	00:29:31.74	-00:45:45.0	22.4	6.6	338.53
2010 GB ₁₇₄	12:38:29.365	+15:02:45.54	25.09 (g)	6.5	347.53
2010 VZ ₉₈	02:08:43.575	+08:06:50.90	20.3 (R)	5.0	313.80
2012 VP ₁₁₃	03:23:47.159	+01:12:01.65	23.1 (r)	4.1	293.97

(3040) Kozai that is perturbed by Jupiter. Another possible Kozai scenario is found when the ratio of semimajor axes (perturbed vs. perturber) is close to one. In that case, the libration occurs at $\omega = 0^\circ$ and 180° ; therefore, the nodes are located at perihelion and at aphelion, i.e. away from the massive perturber (see e.g. Milani et al. 1989). Most studies of the Kozai mechanism assume that the perturber follows an almost circular orbit but the effect is also possible for eccentric orbits, creating a very rich dynamics (see e.g. Lithwick & Naoz 2011). Trujillo & Sheppard (2014) favour a scenario in which the perturber responsible for the possible Kozai libration experimented by 2012 VP₁₁₃ has a semimajor axis close to 250 au. This puts 2012 VP₁₁₃ near or within the co-orbital region of the hypothetical perturber, i.e. the Kozai scenario in which the ratio of semimajor axes is almost one. The Kozai mechanism induces oscillations in both eccentricity and inclination (because for them $\sqrt{1-e^2} \cos i = \text{const}$) and the objects affected will exhibit clustering in both parameters. This is observed in Fig. 3 but the clustering in e could be the result of observational bias (see above).

6 DISCUSSION

Our analysis of the trends observed in Fig. 3 suggests that a massive perturber may be present at nearly 200 au, in addition to the body proposed by Trujillo & Sheppard (2014). The hypothetical object at nearly 200 au could also be in near resonance (3:2) with the one at nearly 250 au (e.g. if one is at 202 au and the other at 265 au, it is almost exactly 3:2). Any unseen planets present in that region must affect the dynamics of TNOs and comets alike. In this scenario, the aphelia, $Q = a(1+e)$, of TNOs and comets (moving in eccentric orbits) may serve as tracers of the architecture of the entire trans-Plutonian region. In particular, objects with $\omega \sim 0^\circ$ or 180° can give us information on the possible presence of massive perturbers in the area because they only experience close encounters near perihelion or aphelion (if the assumed perturbers have their orbital planes close to the fundamental plane of the Solar system). Their perihelia are less useful because so far are < 100 au. However, the presence of gaps in the distribution of aphelia may be a signature of perturbational effects due to unseen planets. Fig. 4 shows the distribution of aphelia for TNOs and comets with semimajor axis greater than 50 au. The top two panels show the entire sample. The two pan-

els at the bottom show the distribution for objects with $\omega < 35^\circ$ or $\omega > 325^\circ$ or $\omega \in (145, 215)^\circ$. These objects have their nodes close to perihelion and aphelion and their distribution in aphelion shows an unusual feature in the range 200–260 au. The number of objects with nodes close to aphelion/perihelion is just 4. The total number of objects with aphelion in that range is 18. Immediately outside that range, the number of objects is larger. Although we may think that the difference is significant, it is unreliable statistically speaking because it could be a random fluctuation due to small number statistics. However, a more quantitative approach suggests that the scarcity is indeed statistically significant. If 18 objects have been found in $\omega \in (0, 360)^\circ$, four within an interval of 140° , and assuming a uniform distribution, we expect seven objects not four. The difference is just 0.8σ . Here we use the approximation given by Gehrels (1986) when $N < 21$: $\sigma \sim 1 + \sqrt{0.75 + N}$. But Fig. 3 indicates that, because of the bias, objects with ω close to 0° or 180° are nearly four times more likely to be identified than those with ω close to 90° or 270° . So, instead of seven objects we should have observed 14 but only four are found, a difference of 2σ , that is marginally significant. Therefore, if they are not observed some mechanism must have removed them.

Fig. 4 (top panels) shows an apparent overall decrease in the number of objects with aphelion in the range 200–300 au. The (e, a) plane plotted in Fig. 5 confirms that the architecture of that region is unlikely to be the result of a gravitationally unperturbed environment. If there are two planets, one at nearly 200 au and another one at approximately 250 au, their combined resonances may clear the area of objects in a fashion similar to what is observed between the orbits of Jupiter and Saturn but see Hees et al. (2014) and Iorio (2014). On the other hand, it can be argued that ETNOs could be the result of close and distant encounters between the proto-Sun and other members of its parent star cluster early in the history of the Solar system (see e.g. Ida, Larwood & Burkert 2000; de la Fuente Marcos & de la Fuente Marcos 2001). However, these encounters are expected to pump up only the eccentricity not to imprint a permanent signature on the distribution of the argument of perihelion in the form of a clustering of values around $\omega=0^\circ$. In addition, they are not expected to induce clustering in inclination.

7 CONCLUSIONS

In this Letter, we have re-examined the clustering in ω found by Trujillo & Sheppard (2014) for ETNOs using a Monte Carlo approach. We confirm that their finding is not a statistical coincidence and it cannot be explained as a result of observational bias. Besides, (90377) Sedna and 2007 TG₄₂₂ are very clear outliers in semimajor axis. We confirm that their presence may signal the existence of a very large population of similar objects. A number of additional trends have been identified here for the first time:

- Observing from the Earth, only ETNOs reaching perihelion at $|\delta| < 24^\circ$ are accessible.
- Besides clustering around $\omega = 0^\circ$, additional clustering in inclination around 20° is observed.
- Asteroids 2003 HB₅₇, 2005 RH₅₂ and 2010 VZ₉₈ all have similar orbits, and their mean longitudes differ by almost 120° . They may be trapped in a 3:2 resonance with an unseen perturber with semimajor axis in the range 195–215 au.
- The orbits of 82158 and 2002 GB₃₂ are very similar. They could be co-orbital to the putative massive object at 195–215 au.
- The study of the distribution in aphelia of TNOs and comets shows a relative deficiency of objects with ω close to 0° or

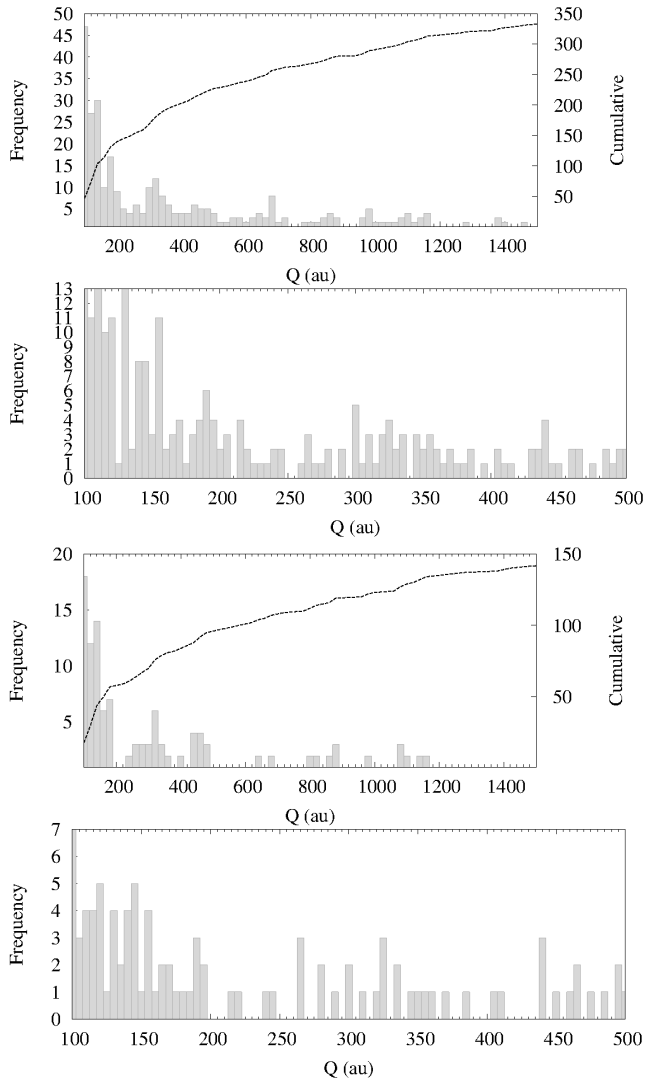


Figure 4. Distribution of aphelia for TNOs and comets with semimajor axis greater than 50 au: all objects (top panels) and only those with $\omega < 35^\circ$ or $\omega > 325^\circ$ or $\eta \in (145, 215)^\circ$ (bottom panels).

180° among those with aphelia in the range 200-260 au. The difference is only marginally significant (2σ), though. Gaps are observed at ~ 205 au and ~ 260 au.

We must stress that our results are based on small number statistics. However, the same trends are found for asteroids and comets, and the apparent gaps in the distribution of aphelia are very unlikely to be the result of Neptune’s perturbations or observational bias. Perturbations from trans-Plutonian objects of moderate planetary size may be detectable by the New Horizons spacecraft (Iorio 2013).

ACKNOWLEDGEMENTS

We thank the anonymous referee for her/his helpful and quick report. This work was partially supported by the Spanish ‘Comunidad de Madrid’ under grant CAM S2009/ESP-1496. We thank M. J. Fernández-Figueroa, M. Rego Fernández and the Department of Astrophysics of the Universidad Complutense de Madrid (UCM) for providing computing facilities. Most of the calculations and part of the data analysis were completed on the ‘Servidor Central

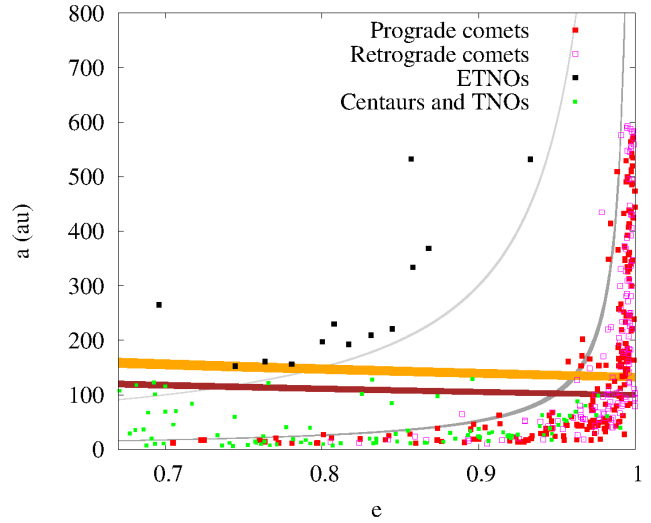


Figure 5. Centaurs, TNOs, ETNOs and comets in the (e, a) plane. The dark gray area represents the eccentricity/semimajor axis combination with periapsis between the perihelion and aphelion of Jupiter, the light gray area shows the equivalent parameter domain if Neptune is considered instead of Jupiter. The brown area corresponds to the (e, a) combination with apoapsis between 190 and 210 au and the orange area shows its counterpart for the range 250–280 au.

de Cálculo’ of the UCM and we thank S. Cano Alsúa for his help during this stage. In preparation of this Letter, we made use of the NASA Astrophysics Data System, the ASTRO-PH e-print server and the MPC data server.

REFERENCES

- Brown M. E., Trujillo C., Rabinowitz D., 2004, *ApJ*, 617, 645
 Brož M., Vokrouhlický D., 2008, *MNRAS*, 390, 715
 de la Fuente Marcos C., de la Fuente Marcos R., 2001, *A&A*, 371, 1097
 de la Fuente Marcos C., de la Fuente Marcos R., 2014a, *MNRAS*, 439, 2970
 de la Fuente Marcos C., de la Fuente Marcos R., 2014b, *MNRAS*, 441, 3, 2280
 Fernández J. A., 2011, *ApJ*, 726, 33
 Gallardo T., Hugo G., Pais P., 2012, *Icarus*, 220, 392
 Gehrels N., 1986, *ApJ*, 303, 336
 Gomes R. S., Matese J. J., Lissauer J. J., 2006, *Icarus*, 184, 589
 Hees A., Folkner W. M., Jacobson R. A., Park R. S., 2014, *Phys. Rev. D*, 89, 102002
 Ida S., Larwood J., Burkert A., 2000, *ApJ*, 528, 351
 Iorio L., 2011, *MNRAS*, 415, 1266
 Iorio L., 2012, *Celest. Mech. Dyn. Astron.*, 112, 117
 Iorio L., 2013, *Celest. Mech. Dyn. Astron.*, 116, 357
 Iorio L., 2014, preprint (arXiv:1404.0258)
 Kozai Y., 1962, *AJ*, 67, 591
 Lithwick Y., Naoz S., 2011, *ApJ*, 742, 94
 Luhman K. L., 2014, *ApJ*, 781, 4
 Lykawka P. S., Mukai T., 2008, *AJ*, 135, 1161
 Matese J. J., Whitmire D. P., 2011, *Icarus*, 211, 926
 Michel P., Thomas F. C., 1996, *A&A*, 307, 310
 Milani A., Carpino M., Hahn G., Nobili A. M., 1989, *Icarus*, 78, 212
 Milani A., Knezevic Z., Novakovic B., Cellino A., 2010, *Icarus*, 207, 769
 Sheppard S. S., Trujillo C., 2014, *MPEC Circ.*, MPEC 2014-F40
 Sheppard S. S. et al., 2011, *AJ*, 142, 98
 Trujillo C. A., Sheppard S. S., 2014, *Nature*, 507, 471

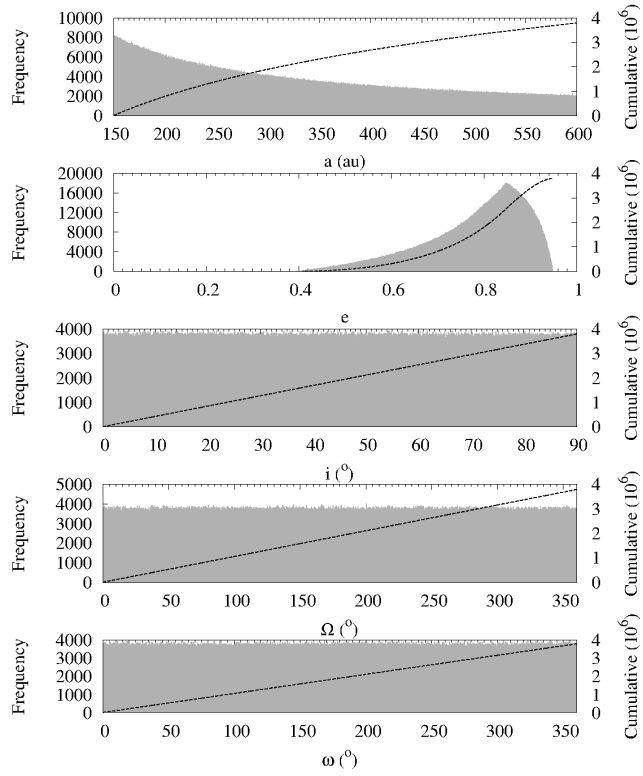


Figure A1. Frequency distributions for the orbital elements of test orbits in Fig. 1. Bin sizes are as in Fig. 3, error bars are too small to be seen.

APPENDIX A: ADDITIONAL FIGURES AND TABLES

Table A1. Various orbital parameters ($\varpi = \Omega + \omega$, $\lambda = \varpi + M$) for the 13 objects discussed in this paper (Epoch: 2456800.5, 2014-May-23.0 00:00:00.0 UT, J2000.0 ecliptic and equinox. Source: JPL Small-Body Database.)

Object	a (au)	e	i ($^\circ$)	Ω ($^\circ$)	ω ($^\circ$)	ϖ ($^\circ$)	λ ($^\circ$)
(82158) 2001 FP ₁₈₅	220.7545067	0.84492276	30.77926	179.32889	6.76597	186.09486	187.24430
(90377) Sedna	532.2664228	0.85696250	11.92861	144.52976	311.18801	95.71777	93.91037
(148209) 2000 CR ₁₀₅	229.9196589	0.80773939	22.70769	128.23495	317.09262	85.32757	90.37358
2002 GB ₃₂	209.4649254	0.83128842	14.18242	177.01044	36.88563	213.89607	213.92324
2003 HB ₅₇	161.1315216	0.76362930	15.49540	197.85952	10.63985	208.49937	209.44502
2003 SS ₄₂₂	197.4196450	0.80023290	16.80405	151.10109	209.98241	1.08350	1.72635
2004 VN ₁₁₂	333.5527773	0.85809672	25.52708	66.04930	327.23428	33.28358	33.55408
2005 RH ₅₂	152.6816879	0.74449569	20.46892	306.19829	32.59337	338.79166	340.86704
2007 TG ₄₂₂	531.9002265	0.93310126	18.57950	112.98155	285.83713	38.81868	39.06830
2007 VJ ₃₀₅	192.3878720	0.81702908	11.98914	24.38420	338.53140	2.91560	4.04033
2010 GB ₁₇₄	368.2345380	0.86809908	21.53344	130.59114	347.52989	118.12103	121.29941
2010 VZ ₉₈	156.4583186	0.78062638	4.50909	117.47040	313.79473	71.26513	68.78231
2012 VP ₁₁₃	264.9446814	0.69599853	24.01737	90.88555	293.97160	24.85715	27.78384